Chicken Egg White—Advancing from Food to Skin Health Therapy: Optimization of Hydrolysis Condition and Identification of Tyrosinase Inhibitor Peptides

Pei-Gee Yap and **Chee-Yuen Gan** *

Analytical Biochemistry Research Centre, Universiti Sains Malaysia, Penang 11800, Malaysia;
peggy-yap@hotmail.com
* Correspondence: cygan@usm.my; Tel.: +60-4653-4206

check for updates

Abstract: Active fragments (bioactive peptides) from the chicken egg white proteins were expected to exert tyrosinase inhibitory activities in which skin hyperpigmentation could be prevented. Egg white was hydrolyzed by trypsin, chymotrypsin and the combination of both enzymes. The enzyme treatments achieved >50% degree of hydrolysis (DH) at substrate-to-enzyme (S/E) ratio of 10–30 (*w/w*) and hydrolysis time of 2–5 h. A crossed D-optimal experimental design was then used to determine the optimal enzyme composition, S/E ratio and hydrolysis time in order to yield hydrolysates with strong monophenolase and diphenolase inhibitory activities. The optimized conditions 55% trypsin, 45% chymotrypsin, S/E 10:1 *w/w* and 2 h achieved 45.9% monophenolase activity inhibition whereas 100% trypsin, S/E 22.13:1 *w/w* and 3.18 h achieved 48.1% diphenolase activity inhibition. LC/MS and MS/MS analyses identified the peptide sequences and the subsequent screening had identified 7 peptides (ILELPFASGDLLML, GYSLGNWVCAAK, YFGYTGALRCLV, HIATNAVLFFGR, FMMFESQNKDLLFK, SGALHCLK and YFGYTGALR) as the potential inhibitor peptides. These peptides were able to bind to H85, H94, H259, H263, and H296 (hotspots for active residues) as well as F92, M280 and F292 (stabilizing residues) of tyrosinase based on structure-activity relationship analysis. These findings demonstrated the potential of egg white-derived bioactive peptides as skin health therapy.

Keywords: bioactive peptide; crossed D-optimal design; diphenolase inhibitory activity; egg white; monophenolase inhibitory activity; pigmentation; tyrosinase

1. Introduction

The excess melanin production and deposition in the melanocytes and keratinocytes cause hyperpigmentation, leading to uneven skin tones. Tyrosinase (E.C. 1.14.18.1) plays a key role in melanin synthesis (melanogenesis) by catalyzing the rate-limiting hydroxylation of L-tyrosine to 3,4-dihydroxy-L-phenylalanine (L-DOPA) and the subsequent oxidation of L-DOPA to dopaquinone, via the monophenolase and diphenolase reactions, respectively [1]. The inhibition of tyrosinase using a nature-derived agent is hence of huge cosmeceutical demand, as some potent skin-lightening ingredients including hydroquinone and heavy metals have been ascribed with harmful side effects and banned for use in certain countries [2,3]. Since the discovery of a potential protein or peptide with tyrosinase inhibitory activity from lemon skin extract in 2006 [4], reports on peptide-based skin lightening agents has increased by leaps and bounds. The anti-pigmentation mechanisms of peptides include tyrosinase inhibition [5], copper chelation [6] and melanogenesis pathway regulation [7]. Peptide was also incorporated as an active ingredient in commercial skin lightening products such as

β-White^TM (contains oligopeptide-68) and Melanostatine^TM 5 (contains nonapeptide-1) marketed by Lucas Meyer Cosmetics. The emergence of bioactive peptides as a new class of therapeutic agent is nonetheless endowed by their relatively small size, low toxicity, fast clearance and high specificity in inhibiting protein-ligand interactions [8].

Anti-pigmentation peptides have been discovered from various natural protein sources including rice bran [6,9] and marine microalgae [10]. Yet, there has been no relevant study on the anti-pigmentation effect of chicken egg white-derived peptides, although this readily available protein has been traditionally used as facial masks to boost skin health. It should be also noted that the active fragments are usually encrypted in the parent protein and required to be released in order to exhibit higher rate of the bioactivity. Enzymatic hydrolysis was therefore employed in this study to release the bioactive peptides from the egg white. In addition, the hydrolysis conditions such as the enzyme used, enzyme composition, substrate-to-enzyme (S/E) ratio and hydrolysis time in order to produce egg white hydrolysates that exhibit the highest monophenolase and diphenolase inhibitory activities should be optimized using D-optimal experimental design. The crossed D-optimal approach conjugates the mixture component (enzyme composition) and process factors (S/E ratio and hydrolysis time) in a single experimental design and generates a relatively smaller number of experimental runs, which has made it more viable in terms of cost and time, especially when each variable comes with multiple levels [11]. In fact, crossed D-optimal design had been successfully implemented to optimize different hydrolysis conditions for other purposes [12,13]. Therefore, this technique was used in this study.

Enzymes used in this study were trypsin and chymotrypsin due to their specific cleavage preferences, i.e., trypsin selectively cleaves at the C-terminal of arginine and lysine [14] whereas chymotrypsin predominantly cleaves at the C-terminal of the aromatic phenylalanine, leucine, methionine, tryptophan and tyrosine [15]. The peptides released may thus fulfil the characteristics of strong tyrosinase inhibitors such as the presence of an aromatic C-terminal residue tyrosine, tryptophan or phenylalanine [9,16] or one or more arginine in combination with phenylalanine, valine, alanine and leucine in the peptide sequence as delineated by Schurink, van Berkel, Wichers and Boeriu [17]. Therefore, the objectives of present study were to determine the optimum hydrolysis conditions of egg white using trypsin and/or chymotrypsin that yield the protein hydrolysates with tyrosinase inhibitory activities followed by peptide sequence identification as well as to investigate the structure-activity relationship between the identified inhibitor peptides and tyrosinase.

2. Materials and Methods

2.1. Chemicals

Egg white powder was purchased from a local market (Penang, Malaysia). Trypsin (EC 3.4.21.4, 10,000 U/mg) and α-chymotrypsin (EC 3.4.21.1, 40 U/mg) from bovine pancreas, tyrosinase (EC 1.14.18.1, 7164 U/mg) from *Agaricus bisporus* were purchased from Sigma-Aldrich. Other chemicals and reagents used were of analytical grade and purchased from Sigma-Aldrich unless otherwise stated.

2.2. Enzymatic Hydrolysis of Egg White Proteins

The enzymatic hydrolysis of egg white was conducted according to the protocol of Miguel, Recio, Gomez-Ruiz, Ramos and Lopez-Fandino [18] with modifications. Briefly, egg white powder was dissolved in 0.05 M sodium phosphate buffer (pH 7.8 or 8.0, depending on the digestive enzyme used) to 5 mg/mL and boiled at 95 °C for 30 min. Subsequently, designated enzyme treatments at various substrate-to-enzyme (S/E) ratios were added to the substrate solution and incubated for different durations at 37 °C with constant shaking of 300 rpm. The details of the experiment will be elaborated in Sections 2.2.1 and 2.2.2. The resultant hydrolysate was then boiled at 95 °C for 30 min to terminate the reaction and centrifuged at 4500× *g* for 15 min. The supernatant was collected and stored at −20 °C until further analysis. Heat-inactivated enzymes were used as the control treatment.

2.2.1. Single-Factor Experiment

The effects of enzyme composition, S/E ratio and hydrolysis time on the degree of hydrolysis (DH) and sodium dodecyl sulphate-polyacrylamide gel electrophoresis (SDS-PAGE) protein band profiling of egg white hydrolysate were studied as preliminary work to investigate the hydrolysis condition required to produce sufficient peptides from egg white. Below are the details of the experiment:

The effect of enzyme composition was investigated based on the hydrolysis of egg white using designated enzyme treatments: 100% trypsin (T), 100% chymotrypsin (C), and 50% trypsin + 50% chymotrypsin (T+C). Phosphate buffer at pH 7.8 was used for T whereas pH 8.0 was used for C and T+C treatments. All these compositions were used for the investigations of the effects of S/E ratio and hydrolysis time. During the investigation of the effect of S/E ratio, the ratio of 10:1, 20:1, 30:1, 40:1 and 50:1 (*w/w*) were studied whereas the hydrolysis time was fixed at 3 h. On the other hand, 0.5, 1, 2, 3, 4 and 5 h were studied during the investigation of the effect of hydrolysis period and the S/E ratio fixed at 30:1 (*w/w*).

The DH of the hydrolysate was determined by measuring the soluble protein content in 10% trichloroacetic acid (TCA) (Fisher Chemicals^{TM}, Leicestershire, UK) according to the protocol of Baharuddin, Halim and Sarbon [19] with modifications. Briefly, the hydrolysate was dissolved in an equal volume of 20% TCA and incubated at room temperature for 30 min. The sample was then centrifuged at 3000× *g* for 10 min. The pellet was suspended in 0.5 mL 0.1 M NaOH and subjected to Bradford assay to determine the amount of soluble protein in the hydrolysate. Briefly, 5 μL of the hydrolysate was added with 250 μL of Bradford reagent and incubated at room temperature for 10 min. The absorbance was then measured at 595 nm using a spectrophotometer (Spectramax M5, Molecular Devices, San Jose, CA, USA). Each measurement was autozeroed against a blank containing Bradford reagent and 0.1 M NaOH. The DH was calculated using the following equation:

$$\text{Degree of hydrolysis (\%)} \;=\; \frac{A_{control} - A_{sample}}{A_{control}} \times 100 \tag{1}$$

where $A_{control}$ denotes the absorbance of the system containing Bradford reagent, NaOH and undigested egg white powder; A_{sample} denotes the absorbance of the system containing Bradford reagent, NaOH and egg white hydrolysate.

To evaluate the protein profile after enzymatic hydrolysis, SDS-PAGE analysis was conducted using 4% stacking gel and 12% resolving gel. Briefly, 10 μL of sample was added with 10 μL 2× Laemmli buffer (Bio-Rad Laboratories Inc., Hercules, CA, USA) and 1 μL 2-mercaptolethanol followed by incubation at 95 °C for 15 min. Then, 10 μL of the mixture was loaded into the well and the set was run at 80 V for15 min followed by 120 V for 1 h. Opti-Protein XL Marker G266 (abm Inc., Richmond, BC, Canada) with a molecular weight range of 10 to 245 kDa was used as the standard protein marker. The gel was stained overnight using staining solution (50% ddH$_2$O, 40% methanol, 10% acetic acid, 0.1% Coomassie Blue) and destained using destaining solution (50% ddH$_2$O, 40% methanol, 10% acetic acid) until blue protein bands were visible against a clear background. The image of the gel was captured using Fujifilm LAS-3000 Imager (Fujifilm, Tokyo, Japan). The molecular weights of the protein bands were analyzed using Multi Gauge software version 3.0 (Fujifilm, Tokyo, Japan).

2.2.2. Optimization of Hydrolysis Conditions for Monophenolase and Diphenolase Inhibitory Activities

Crossed D-optimal design was used to optimize the hydrolysis parameters to yield egg white hydrolysates with the highest tyrosinase inhibitory activities (i.e., the monophenolase inhibitory activity (Y) and diphenolase inhibitory activity (Z)). The enzyme composition (trypsin, X_1; chymotrypsin, X_2) represents the mixture component whereas S/E ratio (X_3) and hydrolysis time (X_4) represents the process factors. Based on the results of single-factor experiment (Section 2.2.1), the levels of the variables were chosen and coded, as shown in Table 1. These variables generated 28 experimental runs. Data analysis and calculation of predicted response were conducted using Design-Expert software

(version 6.0, Minneapolis, MN, USA). Five confirmation experiments were performed to verify the optimized condition.

Table 1. Parameters and levels for crossed D-optimal design of the monophenolase and diphenolase inhibitory activities.

Variable	Coded Variable	Coded Variable Level				
		−1	**−0.5**	**0**	**0.5**	**1**
Trypsin composition (%)	X_1	0	25	50	75	100
Chymotrypsin composition (%)	X_2	0	25	50	75	100
S/E ratio (*w/w*)	X_3	10	15	20	25	30
Hydrolysis time (h)	X_4	2	2.75	3.5	4.25	5

2.3. Determination of Tyrosinase Inhibitory Activities

2.3.1. Monophenolase Inhibitory Activity

The monophenolase inhibitory activity was performed according to Takahashi, Takara, Toyozato and Wada [20] with slight modifications. Briefly, 10 μL of sample and 180 μL of 50 mM potassium phosphate buffer (pH 6.8) containing 0.5 mM L-tyrosine were added to a 96-well plate and incubated at 30 °C for 10 min. The reaction was started by the addition of 1 μL tyrosinase (6250 U/mL) and immediately monitored at 470 nm at every 20 s for 15 min with a constant temperature of 30 °C throughout the reaction. Each measurement was autozeroed against a blank containing L-tyrosine. The monophenolase inhibitory activity is calculated as follows:

$$\text{Monophenolase inhibitory activity (\%)} = \frac{A_{control} - A_{sample}}{A_{control}} \times 100 \tag{2}$$

where $A_{control}$ denotes the absorbance of the system containing tyrosinase and L-tyrosine; A_{sample} denotes the absorbance of the system containing tyrosinase, L-tyrosine and sample.

2.3.2. Diphenolase Inhibitory Activity

The diphenolase inhibitory activity was performed according to Takahashi, Takara, Toyozato and Wada [20] with slight modifications. Briefly, 10μL of sample and 180 μL of 50 mM potassium phosphate buffer (pH 6.8) containing 0.5 mM L-DOPA were added to a 96-well plate and incubated at 30 °C for 10 min. The reaction was started by the addition of 1 μL tyrosinase (6250 U/mL) and immediately monitored at 470 nm at every 10 s for 1 min with constant temperature 30 °C throughout the reaction. Each measurement was autozeroed against a blank containing L-DOPA. The diphenolase inhibitory activity is calculated as follows:

$$\text{Diphenolase inhibitory activity (\%)} = \frac{A_{control} - A_{sample}}{A_{control}} \times 100 \tag{3}$$

where $A_{control}$ denotes the absorbance of the system containing tyrosinase and L-DOPA; A_{sample} denotes the absorbance of the system containing tyrosinase, L-DOPA and sample.

2.4. Identification of Bioactive Peptides

The samples produced using the optimized parameters (Section 2.2.2) were subjected to LC/MS and MS/MS analyses using Easy-nLC II system (Thermo Scientific, San Jose, CA, USA) coupled with LTQ Orbitrap Velos. The chromatographic separation and mass spectrometry (MS) parameters were set up according to Siow and Gan [21]. Data acquisition was conducted using Xcalibur version 2.1. Peptide sequencing and identification based on the spectra acquired were performed using PEAKS Studio version 7.5 (Bioinformatics Solutions Inc., Waterloo, ON, Canada) [22]. The error mass tolerance

allowed for precursor and fragmented ions were 0.1 and 0.8 Da, respectively. Enzyme was not specified in the peaks search against SwissProt2019 database and the false discovery rate (FDR) was estimated with decoy-fusion method. PeptideRanker web server (http://bioware.ucd.ie/, accessed on 6th July 2020) was used to screen for potential biologically active peptides where peptides with PeptideRanker score >0.5 were considered potentially active [23] and hence selected for further analysis. Protein-peptide docking was then performed using PepSite 2 web server (http://pepsite2.russelllab.org/, accessed on 7th July 2020) to predict the potential peptide binding sites on the protein molecule [24]. The server requires inputs for a protein structure in pdb format and a peptide sequence for prediction. The three-dimensional crystal structure of mushroom tyrosinase (PDB ID: 2Y9X) was obtained from the RCSB Protein Data Bank (PDB) at https://www.rcsb.org/ (accessed on 10th July). For peptide sequence input, peptides with >10 residues were split into equal portions since the maximum size of peptide accepted by PepSite 2 server was 10 residues. The predicted protein–peptide binding spots were ranked according to statistical significance where a *p*-value < 0.25 implies significant binding interaction.

2.5. Statistical Analysis

The study was performed in replicates. Statistical analysis was conducted using SPSS version 20.0 (SPSS Institute, Chicago, IL, USA). The results were analyzed using one-way ANOVA. *p*-value less than 0.05 implies a significant difference between sample means. T-test was conducted to analyze the significant ($p < 0.05$) difference between the experimental and predicted results for model validation.

3. Results and Discussion

3.1. Single-Factor Experiment

The SDS-PAGE profile of the protein bands after enzymatic hydrolysis using different enzyme compositions, S/E ratios and hydrolysis times was shown in Figure 1. Generally, protein bands with MW ranging from 11–48 kDa and >245 kDa were observed in control treatments (L1). According to Abdou, Kim and Sato [25], the possible egg white proteins within or near the molecular weight range include ovomucin (230–8300 kDa), ovomacroglobulin (760–900 kDa), ovotransferrin (77.7 kDa), avidin (60 kDa), ovoinhibitor (49 kDa), ovoglobulin G3 (45 kDa), ovalbumin (44.5 kDa), ovoflavoprotein (32–36 kDa), ovoglobulin G2 (36 kDa), ovomucoid (28 kDa), ovoglycoprotein (24.4 kDa), lysozyme (14.4 kDa) and cystatin (12.7 kDa). Ovalbumin-related protein X and Y, on the other hand, share similar molecular weight of 50 kDa [26,27]. Notably, the >245 kDa bands were absent after enzymatic hydrolysis, suggesting the successful cleavage of large molecular weight proteins ovomucin and ovomacroglobulin into smaller protein fragments. For T treatment, the protein bands observed after hydrolysis were <17 kDa (Figure 1a). An 11–17 kDa band was observed at t = 0.5 and 1 h (Figure 1a, Lane 2 and 3) which is likely due to the presence of either lysozyme, cystatin or a subunit (15.6 kDa) of the tetrameric avidin. Protein bands of >25 kDa were also absent as the S/E ratio decreased from 50 to 10 (*w/w*) (Figure 1, Lane 8–12) where S/E 10 (*w/w*) treatment (Figure 1a, Lane 8) showed no observable bands at MW > 11 kDa. A <11 kDa band was found in all hydrolysates regardless of the hydrolysis time and S/E ratio, yet there were no reports on egg white proteins within this molecular weight range. This protein band may be contributed by a new, uncharacterized protein or the hydrolysis product from the aforementioned egg white proteins. Similar observations were recorded in C treatment (Figure 1b) yet 17–48 kDa protein bands were observed at S/E 40 and 50 (*w/w*) (Figure 1b, Lane 11 and 12), suggesting the incomplete hydrolysis of ovalbumin, ovoflavoprotein, ovomucoid or ovoglycoprotein when low amount of enzyme was used. Abeyrathne, Lee, Jo, Nam and Ahn [28] had reported the inability of 1% chymotrypsin to hydrolyze 20 mg/mL ovalbumin even up to 24 h. Apart from incomplete hydrolysis by chymotrypsin, the presence of ovoflavoprotein and ovomucoid could be attributed by their high thermal stability as boiling at 100 °C for 30 min could not denature the protein structures [25,29]. In contrast, T+C treatment showed complete digestion of large MW proteins (25–48 kDa) even when the shortest hydrolysis time at t = 0.5 h (Figure 1c, Lane 2)

and the least amount of enzyme at S/E 50 (*w/w*) (Figure 1c, Lane 12) were used. This implies enzyme combination using trypsin and chymotrypsin was more effective in releasing smaller peptides from large protein molecules compered to individual enzyme treatments.

(**a**)

(**b**)

(**c**)
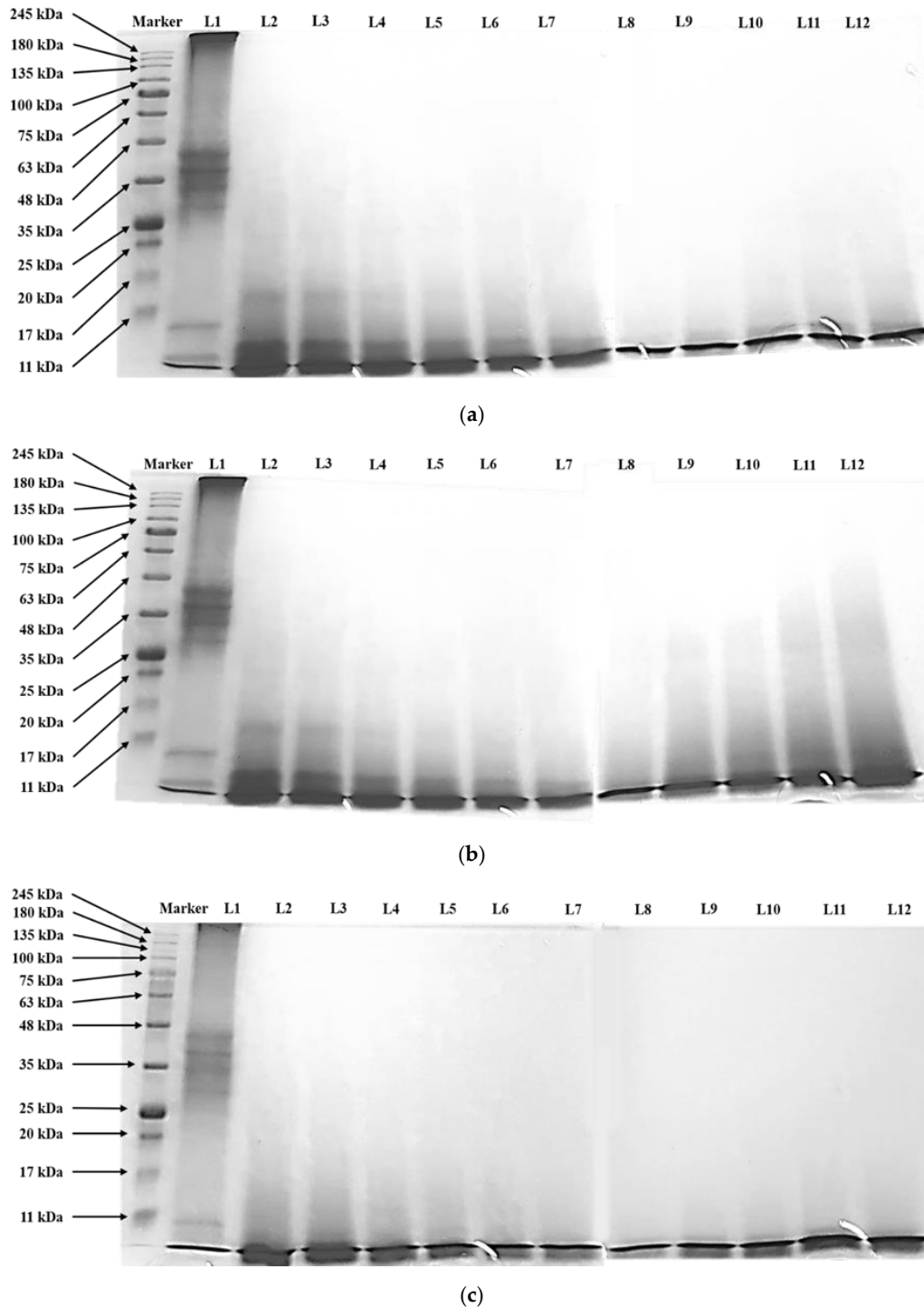
Figure 1. SDS-PAGE protein band profiling of albumin hydrolysate by (**a**) 100% trypsin, T; and (**b**) 100% chymotrypsin, C and (**c**) 50% trypsin + 50% chymotrypsin, T+C treatments at various substrate-to-enzyme (S/E) ratios and hydrolysis times. L1, control; L2, t = 0.5 h; L3, t = 1 h; L4, t = 2 h; L5, t = 3 h; L6, t = 4 h; L7, t = 5 h; L8, S/E = 10 (*w/w*); L9, S/E = 20 (*w/w*); L10, S/E = 30 (*w/w*); L11, S/E = 40 (*w/w*); L12, S/E = 50 (*w/w*).

DH is an indication of peptide bond cleavage in a protein hydrolysate and is vital in modulating the composition and properties of the peptides produced. The effects of different enzyme compositions, S/E ratio and hydrolysis time on the DH of egg white were summarized in Figure 2. Overall, it was observed that a lower S/E ratio and longer hydrolysis time contributed to higher DH in all T, C and T+C enzyme treatments. The highest DH was recorded in the T+C treatments at S/E ratio 10 (88.3 ± 0.4%; Figure 2a) and t = 5 h (86.1 ± 1.7%; Figure 2b). This could be due to the synergistic effect between the trypsin and chymotrypsin as the enzymes have different preferential cleavage sites. For example, the simultaneous treatment with trypsin and chymotrypsin had significantly reduced the time required for total hydrolysis of cheese whey proteins [30]. Chymotrypsin may cleave the bulky side chains of egg white proteins, exposing more cleavage sites for trypsin actions. Moreover, the resistance of albumin to trypsin digestion was overcome by boiling at 95 °C for 30 min before enzymatic hydrolysis. Heat treatment may have partially denatured or altered the tertiary structure of albumin, making the protein more accessible to both trypsin and chymotrypsin cleavage. A high DH corresponds to more peptide production and is often related to high bioactivity. For instance, Noh and Suh [31] who hydrolyzed egg white liquid using Alcalase, Neutrase, Protamex, Flavourzyme, Collupulin and Ficin had reported a positive correlation between DH and antioxidant activity. Alcalase hydrolysate produced at S/E 50 *w/w* and 24 h recorded the highest DH (43.2%) and free radical scavenging effects (82.5%) compared to other enzyme treatments. Moreover, high radical scavenging effect (ORAC value 1193.12 and DPPH value 19.05 Trolox EQ μmol g^{-1}) were recorded when the DH of egg white were higher than 50% [32]. Similar conclusion was drawn by Chen, Chi, Zhao and Xu [33] where the antioxidant and angiotensin I-converting enzyme (ACE) inhibitory activities of egg white protein hydrolysate increased as the DH increased. Thus, together with the SDS-PAGE analysis result, the S/E ratio of 10–30 (*w/w*) and hydrolysis time of 2–5 h were selected for optimization study as these ranges recorded egg white hydrolysates with small peptides (MW < 17 kDa) and DH >50%.
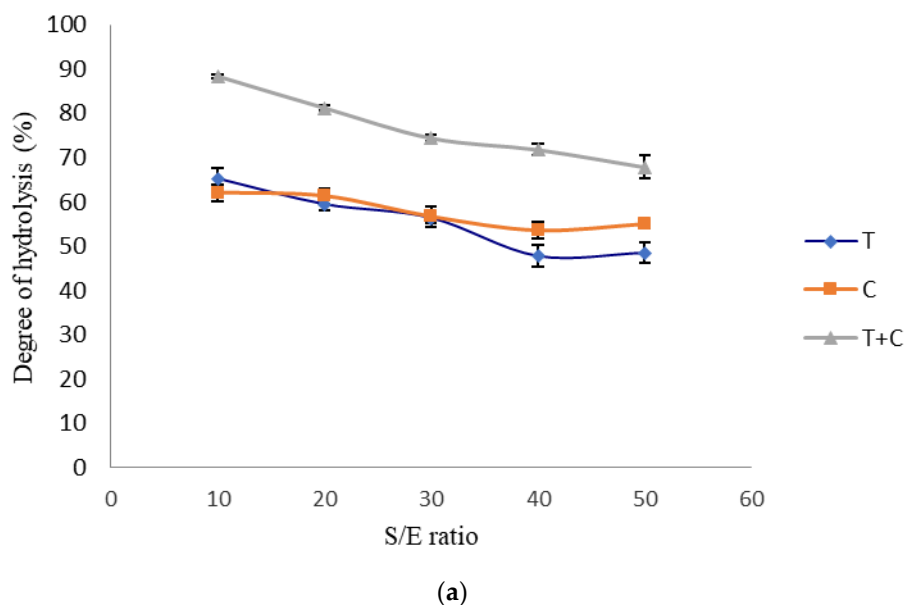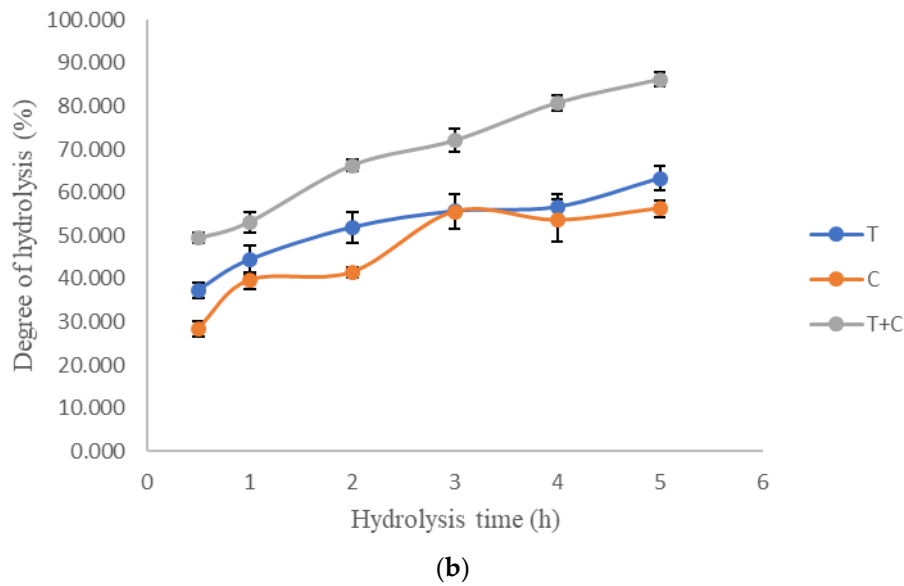

(**a**)

Figure 2. *Cont.*

(**b**)

Figure 2. Effects of enzyme treatments (100% trypsin, T; 100% chymotrypsin, C and 50% trypsin + 50% chymotrypsin, T+C) on the degree of hydrolysis of egg white proteins at various (**a**) substrate-to-enzyme (S/E) ratio where the hydrolysis time is fixed at t = 3 h and (**b**) hydrolysis time where the S/E ratio is fixed at 30 (*w/w*). Results were reported as means with error bars representing the standard deviations of triplicate experiments.

3.2. Optimization of Tyrosinase Inhibitory Activities

The experimental and predicted responses of the 28 generated runs, presented as the mean of triplicate experiments, are shown in Table 2. There was a close agreement between the experimental and predicted responses. X_1 was designated as the slack variable and removed from the model. This is because the summation of X_1 and X_2 equals 100%, hence a significant ($p < 0.05$) X_2 reflects the significance of X_1. Square root transformation of data was performed to normalize the data as suggested by the software.

Table 2. Crossed D-optimal experimental design with the actual and predicted responses for (**a**) monophenolase and (**b**) diphenolase inhibitory activities.

Run	Enzyme Composition (%)		S/E Ratio, X_3	Hydrolysis Time, X_4 (h)	(a) Monophenolase Inhibitory Activity (%)		(b) Diphenolase Inhibitory Activity (%)	
	Trypsin, X_1	Chymotrypsin, X_2			Experimental (y_1)	Predicted * (y_0)	Experimental (z_1)	Predicted # (z_0)
1	100	0	10	5	32.5 ± 2.8	35.6	30.7 ± 1.7	33.6
2	50	50	30	2	20.8 ± 1.8	20.2	44.3 ± 4.5	44.1
3	0	100	20	3.5	15.2 ± 1.4	12.7	31.4 ± 3.5	32.1
4	0	100	10	2	31.6 ± 2.4	30.5	34.2 ± 4.0	33.8
5	100	0	30	2	24.7 ± 1.3	24.3	35.7 ± 2.1	36.1
6	0	100	30	5	39.1 ± 3.4	38.5	40.6 ± 1.8	40.9
7	0	100	30	2	18.9 ± 1.8	19.6	30.2 ± 2.3	31.1
8	100	0	20	2	29.5 ± 4.7	30.7	45.5 ± 3.6	48.1
9	0	100	30	2	20.0 ± 3.8	19.6	32.0 ± 0.5	31.1
10	50	50	10	5	37.2 ± 2.5	37.5	32.8 ± 0.9	31.7
11	0	100	10	2	30.2 ± 5.0	30.5	33.7 ± 1.7	33.8
12	50	50	30	5	26.1 ± 3.7	25.3	28.8 ± 2.7	30.0
13	100	0	30	3.5	26.3 ± 3.5	27.3	38.1 ± 2.4	37.3
14	100	0	10	2	30.3 ± 4.5	32.8	35.8 ± 3.9	35.6
15	50	50	20	2	15.8 ± 3.8	16.9	44.7 ± 3.9	42.5
16	50	50	30	3.5	19.2 ± 2.8	21.0	43.4 ± 3.8	44.3
17	75	25	25	2.75	26.1 ± 3.5	23.5	49.6 ± 3.2	47.0

<div align="center">Table 2. Cont.</div>

Run	Enzyme Composition (%)		S/E Ratio, X_3	Hydrolysis Time, X_4 (h)	(a) Monophenolase Inhibitory Activity (%)		(b) Diphenolase Inhibitory Activity (%)	
	Trypsin, X_1	Chymotrypsin, X_2			Experimental (y_1)	Predicted * (y_0)	Experimental (z_1)	Predicted [#] (z_0)
18	0	100	20	5	21.8 ± 3.6	23.9	36.2 ± 3.4	35.1
19	25	75	15	2.75	19.0 ± 2.1	20.9	31.8 ± 2.5	35.0
20	0	100	30	5	38.4 ± 0.6	38.5	41.6 ± 2.2	40.9
21	0	100	10	5	43.4 ± 4.0	41.5	46.6 ± 2.0	48.7
22	0	100	10	3.5	37.4 ± 4.5	39.7	41.7 ± 2.7	39.3
23	75	25	20	5	48.0 ± 4.1	48.1	35.9 ± 2.8	34.5
24	100	0	30	5	44.7 ± 0.2	44.4	25.0 ± 2.3	25.2
25	100	0	10	5	38.7 ± 0.7	35.6	35.7 ± 4.2	33.6
26	100	0	10	2	35.2 ± 1.3	32.8	36.9 ± 1.4	35.6
27	50	50	10	2	47.2 ± 2.2	45.9	37.7 ± 2.5	38.6
28	75	25	15	3.5	36.1 ± 1.4	34.6	39.1 ± 1.7	39.7

Note: Data is presented as the mean ± standard deviation of triplicate experiments; * predicted using Equation (4); [#] predicted using Equation (5).

Based on Table 2a, the experimental monophenolase inhibitory activity ranged from 15.2–48.0% under various test conditions, with the highest inhibition (47.989%) recorded at $X_1 = 75\%$, $X_2 = 25\%$, $X_3 = 20$ *w/w* and $X_4 = 5$ h. On the other hand, the experimental diphenolase inhibitory activity were ranging from 25.0–49.6% under various test conditions, with the highest inhibition (49.6%) recorded at $X_1 = 75\%$, $X_2 = 25\%$, $X_3 = 25$ *w/w* and $X_4 = 2.75$ h (Table 2b). Analysis of variance (ANOVA) was then conducted to evaluate the significance of the coefficient models at a 95% confidence interval (Table 3). The crossed reduced quadratic × cubic model was selected as it recorded a *p*-value of < 0.0001 for both monophenolase and diphenolase inhibitory activities. The insignificant lack of fit test *p*-value of 0.3348 (Table 3a) and 0.2906 (Table 3b) were observed for monophenolase and diphenolase inhibitory activities, respectively, indicating a well-fitted model that is adequate to describe the observed data. In addition, the values of coefficient of determination, R^2 and adjusted R^2 observed were 0.967 and 0.920, respectively (for monophenolase inhibitory activity), and 0.934 and 0.863, respectively (for diphenolase inhibitory activity), suggesting an excellent fit to the selected model. The coefficient of variation (CV) measures the dispersion of data around the mean. Both models had a low CV of 4.611 and 2.996%, respectively, implying a high precision and low degree of variation of the experiment performed.

Table 3. ANOVA for crossed reduced quadratic × cubic model: estimated regression model of the relationship between the mixture component (X_1, X_2), process variables (X_3, X_4) and the response variables (**a**) monophenolase inhibitory activity (Y) and (**b**) diphenolase inhibitory activity (Z).

Source	Sum of Squares	DF	Mean Square	F Value	Prob > F
(a) Monophenolase inhibitory activity (Y)					
Model	20.668	16	1.292	20.447	<0.0001
X_2	1.678	1	1.678	26.563	0.0003
X_3	0.009	1	0.009	0.139	0.7167
X_4	4.155	1	4.155	65.766	<0.0001
X_2^2	0.075	1	0.075	1.189	0.2988
X_3^2	1.469	1	1.469	23.260	0.0005
X_4^2	0.258	1	0.258	4.079	0.0685
$X_2 X_3$	1.728	1	1.728	27.346	0.0003
$X_2 X_4$	0.973	1	0.973	15.396	0.0024
$X_3 X_4$	0.873	1	0.873	13.812	0.0034
$X_2^2 X_3$	1.489	1	1.489	23.572	0.0005
$X_2^2 X_4$	1.222	1	1.222	19.342	0.0011
$X_2 X_3^2$	5.107	1	5.107	80.846	<0.0001
$X_2 X_4^2$	0.217	1	0.217	3.442	0.0905
$X_3^2 X_4$	2.024	1	2.024	32.038	0.0001

Table 3. *Cont.*

Source	Sum of Squares	DF	Mean Square	F Value	Prob > F
$X_3X_4{}^2$	0.005	1	0.005	0.071	0.7943
$X_2X_3X_4$	0.073	1	0.073	1.148	0.3069
Residual	0.695	11	0.063		
Lack of Fit	0.447	6	0.075	1.507	0.3348
Pure Error	0.247	5	0.049		
Cor Total	21.362	27			
R^2	0.967				
Adjusted R^2	0.920				
C.V.	4.611				
(b) Diphenolase inhibitory activity (Z)					
Model	6.078	14	0.434	13.106	<0.0001
X_2	0.185	1	0.185	5.573	0.0345
X_3	0.071	1	0.071	2.143	0.1669
X_4	0.519	1	0.519	15.658	0.0016
$X_2{}^2$	0.010	1	0.010	0.316	0.5833
$X_3{}^2$	1.283	1	1.283	38.730	<0.0001
$X_4{}^2$	0.214	1	0.214	6.454	0.0246
X_2X_3	0.235	1	0.235	7.104	0.0194
X_2X_4	0.385	1	0.385	11.632	0.0046
X_3X_4	0.258	1	0.258	7.799	0.0152
$X_2{}^2X_3$	0.263	1	0.263	7.939	0.0145
$X_2{}^2X_4$	1.060	1	1.060	31.990	<0.0001
$X_2X_3{}^2$	1.771	1	1.771	53.473	<0.0001
$X_3X_4{}^2$	0.314	1	0.314	9.481	0.0088
$X_2X_3X_4$	0.040	1	0.040	1.198	0.2936
Residual	0.431	13	0.033		
Lack of Fit	0.315	8	0.039	1.696	0.2906
Pure Error	0.116	5	0.023		
Cor Total	6.508	27			
R^2	0.934				
Adjusted R^2	0.863				
C.V.	2.996				

The significant ($p < 0.05$) effect on the monophenolase inhibitory activity was contributed by the linear terms X_4 and X_2, quadratic term $X_3{}^2$ and various interaction terms X_2X_3, X_2X_4, X_3X_4, $X_2{}^2X_3$, $X_2{}^2X_4$, $X_2X_3{}^2$ and $X_3{}^2X_4$, whereas, the significant ($p < 0.05$) effect on the diphenolase inhibitory activity was contributed by the linear terms X_4 and X_2, quadratic terms $X_3{}^2$ and $X_4{}^2$ alongside various interaction terms X_2X_3, X_2X_4, X_3X_4, $X_2{}^2X_3$, $X_2{}^2X_4$, $X_2X_3{}^2$ and $X_3X_4{}^2$. This suggested the hydrolysis time, enzyme compositions, as well as their interactions with S/E ratio, played a prominent role in the inhibition of these activities. To better fit the model, backward elimination step was carried out to eliminate the non-significant terms. The final response equations for monophenolase and diphenolase inhibitory activities in coded variables are given in Equations (4) and (5), respectively.

$$\sqrt{Monophenolase\ inhibitory\ activity} = 6.269 - 2.711x_2 + 1.395x_4 - 1.084x_3^2 + 0.612x_4^2 - 3.157x_2x_3$$
$$- 2.128x_2x_4 + 0.289x_3x_4 + 2.835x_2^2x_3 + 2.334x_2^2x_4 + 3.45x_2x_3^2 \quad (4)$$
$$- 0.926x_2x_4^2 - 0.938x_3^2x_4$$

$$\sqrt{Diphenolase\ inhibitory\ activity} = 6.943 - 1.258x_2 - 0.269x_4 - 0.952x_3^2 - 0.269x_4^2 + 1.301x_2x_3$$
$$- 1.472x_2x_4 - 0.139x_3x_4 - 1.267x_2^2x_3 + 2.244x_2^2x_4 + 1.726x_2x_3^2 \quad (5)$$
$$- 0.226x_3x_4^2$$

3.3. Verification of Predictive Models

Various combination of hydrolysis parameters was suggested to verify the suitability of the predictive models. Taking into consideration the cost, efficiency and feasibility of the experiment, the optimal condition (desirability value of 0.949, which indicating that the suggested condition is close to the desired process condition-minimum amount of enzymes, minimum hydrolysis time and maximum inhibitory activities) to achieve monophenolase inhibitory activity of 45.9% corresponded to 55% trypsin, 45% chymotrypsin, S/E ratio 10:1 (*w/w*) and hydrolysis time 2 h was examined. The experimental value of 45.3% was found close with no significant ($p > 0.05$) difference with the predicted value (45.9%). The DH determined was 84.8 ± 1.8%. For diphenolase inhibitory activity, the optimal condition suggested was 100% trypsin, 0% chymotrypsin, S/E ratio 22.13:1 (*w/w*) and hydrolysis time 3.18 h. The experimental value of 48.1% was found close with no significant ($p > 0.05$) difference with the predicted value (48.1%). The degree of hydrolysis determined was 64.0 ± 2.1%. Therefore, this model was valid for the optimization of monophenolase and diphenolase inhibitory activities from egg white. It was also observed that in monophenolase inhibitory activity optimization, even though 48.0% was achieved by sample run 23 (Table 2), 5 h of hydrolysis time was required, whereas 2 h of hydrolysis time could achieve 45.3% (the difference by only 2.7%) in the optimized condition. In the optimization of diphenolase inhibitory activity, the optimized sample achieved 48.1% activity by using only trypsin (lower in cost) compared to the sample run 17 (49.6%) in which the difference was only 1.5%. Therefore, it was suggested that the optimization process had managed to achieve the goal of study.

3.4. Identification of Bioactive Peptides

There were 139 and 189 peptides identified for monophenolase and diphenolase inhibitory activities, respectively, using PEAKS Studio (Appendix A Table A1). For monophenolase inhibitory activity, 76, 36, 4, 7, 11, 4 and 1 peptides were identified from ovalbumin, ovotransferrin, ovomucoid, ovalbumin-related protein X, ovalbumin-related protein Y, Ovomucin, and cystatin, respectively, where they were found to achieve 77%, 45%, 42%, 38%, 32%, 16% and 12% coverages of the corresponding protein sequences (Appendix A Table A1a). For diphenolase activity, 81, 54, 9, 12, 4, 8, 20 and 2 peptides identified were found to match 81%, 63%, 54%, 38%, 29%, 28%, 26% and 2% sequence coverages of ovalbumin, ovotransferrin, lysozyme, ovomucoid, ovalbumin-related protein X, ovalbumin-related protein Y, Ovomucin and ovostatin, respectively (Appendix A Table A1b). Subsequently, PeptideRanker web server was used to screen for potential biologically active peptides since the likeliness of being bioactive is usually governed by specific structural characteristics of peptide [23]. The use of PeptideRanker for initial screening and prediction had been proven successful to identify bioactive peptides with wide array of bioactivities [34–36]. Therefore, there were 7 and 21 peptides (PeptideRanker score >0.5) shortlisted for monophenolase and diphenolase inhibitory activities, respectively. The shortlisted peptides were further subjected to structure-activity relationship analysis with mushroom tyrosinase using the PepSite2 web server.

The *p*-values of mushroom tyrosinase-peptide binding interactions predicted by PepSite 2 web server were summarized in Table 4. A smaller *p*-value signifies higher potential of peptide binding to the enzyme. The smallest *p*-value was recorded by ADHPF (0.002658), AFKDEDTKAMPF (0.02053) and ILELPFASGDLLML (0.03464) whereas the largest *p*-value was recorded by DGSGGCIPK (0.1274) for monophenolase inhibitory activity (Table 4a). For diphenolase activity, SDFHLFGPPGK (0.009412), FDGRSR (0.01312) and FNCSSAGPGAIGSEC (0.01614) were among the peptides with the smallest *p*-values whereas YFGYTGALR had recorded the largest *p*-value of 0.2364 (Table 4b). Overall, all peptides showed significant ($p < 0.25$) binding interactions with mushroom tyrosinase. Notably, phenylalanine, leucine and alanine were frequently observed in the peptide sequences. Phenylalanine may act as the pseudo-substrate of tyrosinase since it is structurally identical to tyrosine, the natural substrate of tyrosinase. Besides, the hydrophobic side chains of leucine and alanine may interact directly with the hydrophobic binding pocket of tyrosinase to cause enzyme inhibition. According to

Strothkamp, Jolley and Mason [37], mushroom tyrosinase is a tetramer comprising of two H subunits and two L subunits. The L subunit is the product of *Orf239342* gene and possesses a lectin-like structure, hence annotated as mushroom tyrosinase associated lectin-like protein. It comprises residues 9–28 and 35–150 of ORF239342 protein and is arranged into 12 antiparallel β-strands that is located away from the tyrosinase catalytic site, suggesting an insignificant role in enzyme activity [38]. The L subunit was postulated to provide innate immunity against bacterial infection [39] and act as a cofactor in melanin production [40]. In contrast, the H subunit originates from *ppo3* gene and covers residues 2–392 of PPO3. This subunit is made up of 13 α-helices, 8 short β-strands and loops that structured the catalytically essential tyrosinase core domain [38,41]. The H subunit houses a binuclear copper active site where copper A is coordinately bonded with H61, H85 and H94 whereas copper B to H 259, H263 and H296. The 6 histidine residues form a hydrophobic binding pocket at the bottom of the H subunit and H263 is postulated to regulate proper orientation of incoming substrate [38]. The structural rigidity of the binding pocket is maintained by several interactions between the 6 histidine and their neighboring residues. For instance, the side chain rotational freedom of H85 is restricted through the formation of a thioether bond with the side chain of C83. This thioether bond stabilizes H85 and is also suggested to optimize redox potential as well as to facilitate rapid electron transfer for the redox reactions occurring in the binuclear copper site [38,42]. Furthermore, the presence of F90 confers structural constraints to H94, H259 and H296 while F292 limits the side chain flexibility of H61, H263 and H296 [38]. The interaction between M280 and the aromatic ring of histidines also stabilizes the protein structure [43] and this residue may aid in copper incorporation into the binding pocket [44]. Notably, the ILELPFASGDLLML for monophenolase inhibitory activity (Table 4a) and GYSLGNWVCAAK, YFGYTGALRCLV, HIATNAVLFFGR, FMMFESQNKDLLFK, SGALHCLK and YFGYTGALR for diphenolase inhibitory activity (Table 4b) were found to interact with H61, H85, H94, H259, H263, and H296 (hotspot residues) and F92, F292 and M280 (stabilizing residues) of mushroom tyrosinase. The peptide interactions with the hotspot residues may weaken or hinder enzyme binding with its putative substrate whereas peptide interactions with the stabilizing residues may disrupt the integrity of active site, which reduces the catalytic potency of the enzyme. Thus, ILELPFASGDLLML, GYSLGNWVCAAK, YFGYTGALRCLV, HIATNAVLFFGR, FMMFESQNKDLLFK, SGALHCLK and YFGYTGALR represent potential tyrosinase inhibitory peptides.

Table 4. List of potential biologically active egg white-derived peptides shortlisted for (**a**) monophenolase and (**b**) diphenolase inhibitory activities using PeptideRanker web server and their potential binding sites on mushroom tyrosinase predicted using PepSite 2 web server.

No.	Peptide Sequence	Egg Protein Fragment	Peptide Length	Potential Binding Sites of Mushroom Tyrosinase (PDB ID: 2Y9X)	PepSite 2 *p*-Value
(a) Monophenolase inhibitory activity				
1	ADHPF	Ovalbumin	5	Y140, K389, H390	0.002658
2	AFKDEDTKAMPF	Ovalbumin	12	N22, F135, D137, Y140. R301, P366, D367, W386, H390, Y391	0.02053
3	ILELPFASGDLLML	Ovalbumin-related protein X	14	Y36, L40, F54, G58, **H61**, **H85**, F90, **H94**, W101, Q133, **H259**, **H263**, *M280*, H285, A286, A287, F288, D289, P290, *F292*, W293, **H296**	0.03464
4	DKLPGFGD	Ovalbumin	8	Y140, P370, Y382, W386, K389, H390	0.05277
5	FDKLPGFGD	Ovalbumin	9	Y140, P370, Y382, W386, K389, H390	0.0722
6	FDKLPGFGDSIEAQCGTSVN	Ovalbumin	20	Y140, T233, R301, M309, D367, P370, Y382, N384, W386, H388, K389, H390	0.08107
7	DGSGGCIPK	Ovomucin	9	N22, F135, D137, Y140, R301, D367, Y382, W386, K389, H390	0.1274
(b) Diphenolase inhibitory activity				
1	SDFHLFGPPGK	Ovotransferrin	11	Y140, R301, D367, Y382, W386, H390	0.009412
2	FDGRSR	Ovomucin	6	D137, R301, P366, D367, W386, H390, Y391	0.01312
3	FNCSSAGPGAIGSEC	Ovomucin	15	N22, F135, D137, Y140, R301, P366, D367, W386, H390, Y391	0.01614
4	MYQIGLFR	Ovalbumin	8	D137, Y140, R301, D367, P370, Y382, W386, H390, Y391	0.01832
5	GYSLGNWVCAAK	Lysozyme	12	**H61**, N81, Y82, C83, T84, **H85**, F90, W93, **H94**, R95, Y97, E98, E256, **H259**, **H263**, **M280**, V283, A286, A287, **F292**, W293, **H296**	0.01891
6	DLLFKDSAIMLK	Ovotransferrin	12	D137, Y140, R301, D367, Y382, W386, K389, H390, Y391	0.02538
7	CQLCQGSGGIPPEK	Ovotransferrin	14	D137, Y140, R301, P366, D367, Y382, W386, H390, Y391	0.02578
8	ADHPFLF	Ovalbumin	7	Y140, R301, P366, D367, F368, P370, W386, H390	0.03051
9	SGAFHCLK	Ovotransferrin	8	Y140, Y382, W386, H390	0.03994
10	YFGYTGALRCLV	Ovotransferrin	12	**H61**, **H85**, **H94**, Y97, Y140, **H259**, **H263**, *M280*, V283, A287, *F292*, W293, H295, **H296**, V299, R301, D367, Y382, W386, H390	0.04488
11	HIATNAVLFFGR	Ovalbumin	12	G58, **H61**, C83, **H85**, F90, Typ93, **H94**, Y97, D137, Y140, **H259**, **H263**, *M280*, H285, A286, A287, F288, D289, *F292*, W293, **H296**, R301, D367, W386, H390, Y391	0.04707
12	FKDEDTQAMPFR	Ovalbumin	12	D137, Y140, R301, P366, D367, W386, H390, Y391	0.05594

Table 4. *Cont.*

No.	Peptide Sequence	Egg Protein Fragment	Peptide Length	Potential Binding Sites of Mushroom Tyrosinase (PDB ID: 2Y9X)	PepSite 2 *p*-Value
			(a) Monophenolase inhibitory activity		
13	FMMFESQNKDLLFK	Ovotransferrin	14	**H61**, N81, Y82, C83, T84, **H85**, F90, W93, **H94**, Y97, D137, Y140, **H259**, **H263**, *M280*, A286, A287, *F292*, W293, **H296**, R301, P366, D367, W386, H390, Y391	0.06287
14	FDKLPGFGD	Ovalbumin	9	Y140, P370, Y382, W386, K389, H390	0.0722
15	SMLVLLPDEVSGLEQLESIINFEK	Ovalbumin	24	D137, Y140, R301, D367, P370, Y382, W386, K389, H390, Y391	0.08195
16	SGYSGAFHCLK	Ovotransferrin	11	Y140, R301, P366, D367, Y382, W386, H390	0.0849
17	SGGQFSLTSTVKVC	Ovomucin	14	D137, Y140, R301, D367, W386, H390, Y391	0.08667
18	SGALHCLK	Ovotransferrin	8	**H61**, N81, Y82, C83, T84, **H85**, W93, **H94**, R95, Y97, E98, **H259**, **H263**, A286, A287, *F292*, W293, **H296**	0.1247
19	SSCICS	Ovomucin	6	N22, F135, D137, R301, P366, D367, W386, H390	0.1938
20	SSCEDCVCT	Ovomucin	9	D137, Y140, R301, D367, W386, H390, Y391	0.2086
21	YFGYTGALR	Ovotransferrin	9	**H61**, **H85**, **H94**, Y97, **H259**, **H263**, *M280*, V283, A286, Als287, *F292*, W293, H295, **H296**, V299	0.2364

Note: Underlined residues are actively involved in binding interaction with mushroom tyrosinase; Residues in bold indicate mushroom tyrosinase hotspots; Residues in italics indicate stabilizing residues.

On the other hand, majority of the peptides were also found to bind to Y140, W386 and H390 (Table 4) which were not within the mushroom tyrosinase substrate binding pocket. Hassani Hagnbeen and Fazli [45] reported two mixed-type inhibitors of tyrosinase, phthalic acid and cinnamic acid, each bound to different binding sites of the enzyme. For instance, phthalic acid formed hydrogen bonds with W136, W141 and G149 and van der Waals interactions with D137, W138, G139, Y140, F147 and F224 whereas cinnamic acid form hydrogen bonds with Q307 and D312 and van der Waals interactions with T308, Y311, V313, Y314, E356 and W358. Jung et al. [46] also reported a mixed-type tyrosinase inhibitor, (E)-2-(2,4-dihydroxybenzylidene)-2,3-dihydro-1H-inden-1-one (BID3) which formed a hydrogen bond with Y140 and interacted hydrophobically with L24, F147 and I148. These findings suggest potential peptide interaction with non-specific binding site of the enzyme since the allosteric site of mushroom tyrosinase has yet to be identified.

4. Conclusions

In this study, egg white has been proven to be more than just a food component. The optimization of enzymatic hydrolysis conditions, LC/MS MS/MS peptide identification and sequencing followed by structure-activity relationship analyses had corroborated the potential of this food protein as a source for the production of anti-tyrosinase peptides to prevent skin hyperpigmentation. Nonetheless, the monophenolase and diphenolase inhibitory peptides identified will next be chemically synthesized and validated for their in vitro anti-tyrosinase efficacies before proceeding to in vivo assays to examine their effects on the melanogenesis pathway regulatory proteins.

Appendix A

Table A1. List of egg white-derived peptides for (**a**) monophenolase and (**b**) diphenolase inhibitory activities with their corresponding PeptideRanker scores.

No.	Egg Protein Sequence Coverage	Peptide	Peptide Sequence Number	Score
		(a) Monophenolase inhibitory activity		
1		ADHPF *	361–365	0.8592
2		FDKLPGFGD *	60–68	0.6817
3		FDKLPGFGDSIEAQCGTSVN *	60–79	0.5429
4		AFKDEDTKAMPF *	188–199	0.5332
5		DKLPGFGD *	61–68	0.5174
6		MSALAM	36–41	0.4941
7		RGGLEPINF	127–135	0.4842
8		YPILPEYL	112–119	0.4732
9		AFKDEDTQAMPF	188–199	0.4636
10		VLLPDEVSGLEKLESIINF	244–262	0.4494
11		QVLLPDEVSGLEQLESIINF	243–262	0.4335
12		KDEDTQAMPF	190–199	0.4113
13		FDKLPGFGDSIEAQ	60–73	0.4067
14		YPILPEYLQCVKELY	112–126	0.3960
15		VLLPHEVSGLEQLESIINF	244–262	0.3712
16		LVQLPDEVSGLEQLESIINF	243–262	0.3593
17		LPDEVSGLEQLESIINF	246–262	0.3544
18		MAMGITDVF	299–307	0.3250
19		SSSANLSGISSAESLK	308–323	0.3207

Table A1. *Cont.*

No.	Egg Protein Sequence Coverage	Peptide	Peptide Sequence Number	Score
		(a) Monophenolase inhibitory activity		
20		LVLLPDEVSGLEQLESIINF	243–262	0.3189
21		VHHANENIFY	21–30	0.3132
22		VTEQESKPVQMMYQIGLF	210–218	0.3126
23		VHHANENIF	21–29	0.2953
24		GGLEPINFQTAADQAR	128–143	0.2810
25		VLLPDEVSGLEQLESIINFE	244–263	0.2738
26		VASMASEKMK	220–229	0.2728
27		AAHAEINEAGR	330–340	0.2679
28		AEERYPILPEYL	108–119	0.2648
29		YPILPEYLQ	112–120	0.2638
30		ISQAVHAAHAEINEAGR	324–340	0.2599
31		SANLSGISSAESLK	310–323	0.2537
32		SWVESQTNGIIR	148–159	0.2523
33		AFKDEDTQAMP	188–198	0.2456
34		SGISSAESLK	314–323	0.2242
35		MAMGITDVFSSSANLSGIS	299–317	0.2239
36		INSWVESQTNGIIR	146–159	0.2193
37		LYAEERYPILPEYL	106–119	0.2015
38		SGISSAESL	314–322	0.1982
39		VLLPDEVSGLEQLESIINFEK	244–264	0.1885
40		VLQPSSVHSQTAM	161–173	0.1836
41		VLLPDEVSGLEQL	244–256	0.1835
42		LSGISSAESLK	313–323	0.1793
43		HAEINEAGR	332–340	0.1789
44		SAEAGVDAASVSEEF	345–359	0.1784
45		VLLPDEVSGLEQLESIIN	244–261	0.1723
46		EVVGSAEAGVDAASVSEEFR	341–360	0.1703
47		NVLQPSSVHSQTAM	160–173	0.1699
48		AMGITDVFSS	300–309	0.1674
49		SSNVMEE	270–276	0.1638
50		EVVGSAEAGVDAASVSEEF	341–359	0.1629
51		SGISSAESLQ	314–323	0.1544
52		ELINSWVESQTNGIIR	144–159	0.1482
53		SGISSAESLE	314–323	0.1469
54		VTEQESKPVQMM	201–212	0.1453
55		AEINEAGR	333–340	0.1437
56		VLKPSSVDSQTAM	161–173	0.1431
57		VESQTNGIIR	150–159	0.1401
58		NVLQPSSVDSQTAM	160–173	0.1362
59		VLLPDEVSGLEQLESR	244–259	0.1282
60		VLLPDEVSGLEKLESIINFEK	244–264	0.1189
61		VASMASEK	220–227	0.1086
62		ISQAVH	324–329	0.1070
63		TSSNVMEER	269–277	0.1050
64		VLLPHEVSGLEQLES	244–258	0.0986
65		QITKPNDVY	90–98	0.0968
66		DILNQITKPNDVY	86–98	0.0951
67		VLLPDEVSGLEQLES	244–258	0.0916
68		NQITKPNDVY	89–98	0.0879
69		LTEWTSSNVMEER	265–277	0.0807
70		VTEQESKPVQMK	201–212	0.0805
71		RVTEQESKPVQM	200–211	0.0787
72		NQITEPNDVY	89–98	0.0742
73		VTEQESKPVQM	201–211	0.0712
74		VTEQESKPV	201–209	0.0395
75		NVLQPSSVDSQTAMVLVNAIVFK	160–182	0.0365
76		NVLQPSSVDSQTAMVLVNAIVF	160–181	0.0218
77		KDSNVNWNNLK	458–468	0.4863
78		GEADAVALHGGLVY	406–419	0.4290
79		NLQMDDFELL	579–588	0.4262
80		NLKMDDFELL	579–588	0.3988

Table A1. *Cont.*

No.	Egg Protein Sequence Coverage	Peptide	Peptide Sequence Number	Score
(a) Monophenolase inhibitory activity				
81		KDQLTPSPR	352–360	0.3329
82		VPSLMHSQLY	329–338	0.3155
83		GAIEWEGIESGSVEKAVAK	155–173	0.2986
84		KGEADAVALDGGLVY	405–419	0.2793
85		TAGVCGLVPVMAER	420–433	0.2662
86		VPSLMDSQLY	329–338	0.2612
87		AQSDFGVDTK	289–298	0.2525
88		GAIEWEGIESGSVEQAVAK	155–173	0.2308
89		RVPSLMDSQLY	328–338	0.2249
90		VPVMAER	427–433	0.1784
91		VAAHAVVAR	266–274	0.1704
92		GAIEWEGIESGSVEQAVAE	155–173	0.1683
93		AIEWEGIESGSVEQAVAK	156–173	0.1624
94		LKPIAAEVY	93–101	0.1209
95		KLKPIAAEVY	92–101	0.1184
96		HAVVVRPEK	611–619	0.1049
97		IQHSTVEENTGGK	559–571	0.1005
98		TVNDLQGK	124–131	0.0955
99		AVVVRPEK	612–619	0.0953
100		TVNENAPDQKDEYELL	231–246	0.0946
101		QGIESGSVEQAVAK	160–173	0.0919
102		TDERPASY	443–450	0.0891
103		IKHSTVEENTGGK	559–571	0.0865
104		VAAHAVVARDDNQVEDIW	266–283	0.0847
105		DLTQQER	44–50	0.0846
106		VQHSTVEENTGGK	559–571	0.0835
107		EGIESGSVEQAVAK	160–173	0.0768
108		TVISSLK	682–688	0.0710
109		HTTVNENAPDQKDEYELL	229–246	0.0630
110		EGIESGSVEQAVAE	160–173	0.0600
111		VVVRPEK	613–619	0.0580
112		TVEENTGGK	563–571	0.0491
113		ISDAVHGVF	324–332	0.4692
114		MISDAVHGVF	323–332	0.4224
115		VLLPDEVSGLEHIEKTINF	244–262	0.2846
116		HSLELEEFR	354–362	0.2286
117	Ovalbumin-related protein Y (32%)	SLEIADKLY	99–107	0.1898
118		VLLPDEVSGLER	244–255	0.1871
119		VLLPDEVSGLERIEKTIN	244–261	0.1605
120		VLLPDEVSGLERIEK	244–258	0.1316
121		MEVNEEGTEATGSTGAIGNIK	333–353	0.1211
122		TGGVEEVNFK	127–136	0.1200
123		NVATLPAEK	219–227	0.1152
124		ILELPFASGDLLML *	74–87	0.8643
125		TGISSAESLK	158–167	0.1223
126	Ovalbumin-related protein X (38%)	NVATLPAEK	63–71	0.1152
127		VLLPDEVSDLER	88–99	0.1084
128		ISQAVH	168–173	0.1070
129		AGSTGVIEDIK	187–197	0.1025
130		VTKQESKPVQM	45–55	0.0833
131		FPNATDKEGK	32–41	0.3269
132	Ovomucoid (42%)	DLRPICGTDGVTY	49–61	0.2154
133		VEQGASVDKR	137–146	0.0903
134		VEQGASVDER	137–146	0.0734
135		DGSGGCIPK *	814–822	0.6103
136	Ovomucin (16%)	VTDSF	1591–1595	0.2004
137		SNSLVILTQA	1494–1503	0.1384
138		IQEIATDPGAEK	941–952	0.1215
139	Cystatin (12%)	LLGAPVPVDENDEGLQR	30–46	0.2450

Table A1. *Cont.*

No.	Egg Protein Sequence Coverage	Peptide	Peptide Sequence Number	Score
		(b) Diphenolase inhibitory activity		
1		ADHPFLF *	361–367	0.9699
2		MYQIGLFR *	212–219	0.8011
3		SMLVLLPDEVSGLEQLESIINFEK *	241–264	0.6983
4		FDKLPGFGD *	60–68	0.6817
5		HIATNAVLFFGR *	371–382	0.5209
6		FKDEDTQAMPFR *	189–200	0.5001
7		DEDTKAMPFR	191–200	0.4978
8		ILELPFASGTMS	230–241	0.4972
9		DEDTQAMPFR	191–200	0.4842
10		MLVLLPDEVSGLEQLESIINFEK	242–264	0.4842
11		YPILPEYLQCVK	112–123	0.4769
12		AFKDEDTQAMPFR	188–200	0.4702
13		SSSANLSGISSAESLK	308–323	0.3207
14		SQAVHAAHAEINEAGR	325–340	0.2965
15		VTEQESKPVQMMYQIGLFR	201–219	0.2886
16		GGLEPINFQTAADQAR	128–143	0.2810
17		SQTAMVLVNAIVFK	169–182	0.2781
18		VASMASEKMK	220–229	0.2728
19		AAHAEINEAGR	330–340	0.2679
20		YPILPEYLQ	112–120	0.2638
21		QAVHAAHAEINEAGR	326–340	0.2606
22		ISQAVHAAHAEINEAGR	324–340	0.2599
23		EAQCGTSVNVHSSLR	71–85	0.2554
24		SANLSGISSAESLK	310–323	0.2537
25		SSANLSGISSAESLK	309–323	0.2497
26		EVCGSAEAGVDAASVSEEFR	341–360	0.2424
27		GLEPINFQTAADQAR	129–143	0.2420
28		VLLPDEVSGLEQLESIINFEQ	244–264	0.2410
29		VLVNANVFK	174–182	0.2362
30		NSQAVHAAHAEINEAGR	324–340	0.2273
31		ISQAVHAAHAEIN	324–336	0.2267
32		DILNQITKPNDVYSFSLASR	86–105	0.2229
33		FQTAADQAR	135–143	0.2202
34		VLVNAIVFK	174–182	0.2049
35		MAMGITDVFSSSANLSGISSAESLK	299–323	0.1963
36		AVHAAHAEINEAGR	327–340	0.1935
37		SVNVHSSLR	77–85	0.1930
38		LCEWTSSNVMEER	265–277	0.1886
39	Ovalbumin (81%)	VLLPDEVSGLEQLESIINFEK	244–264	0.1885
40		DLEPINFQTAADQAR	129–143	0.1854
41		LSGISSAESLK	313–323	0.1793
42		HAEINEAGR	332–340	0.1789
43		LEPINFQTAADQAR	130–143	0.1739
44		EVVGSAEAGVDAASVSEEFR	341–360	0.1703
45		DILNQITKPNDVYSF	86–100	0.1698
46		EAGVDAASVSEEFR	437–360	0.1664
47		AEAGVDAASVSEEFR	346–360	0.1641
48		VHAAHAEINEAGR	328–340	0.1633
49		EVVGAAEAGVDAASVSEEFR	341–360	0.1628
50		EPINFQTAADQAR	131–143	0.1588
51		ISQAVHAAH	324–332	0.1572
52		ELINSWVESQTNGIIR	144–159	0.1482
53		VTEQESKPVQMM	201–212	0.1453
54		VTEQESKPVQMMY	201–213	0.1416
55		RVTEQESKPVQMMY	200–213	0.1413
56		GITHVFSSSANLSGISSAESLK	302–323	0.1401
57		VLVNAIVFE	174–182	0.1401
58		AMGNTDVFSSSANLSGISSAESLK	300–323	0.1395
59		NVLQPSSVDSQTAM	160–173	0.1362
60		EWTSSNVMEER	267–277	0.1280

Table A1. *Cont.*

No.	Egg Protein Sequence Coverage	Peptide	Peptide Sequence Number	Score
		(b) Diphenolase inhibitory activity		
61		GTSVNVHSSLR	75–85	0.1274
62		LQPSSVDSQTAMVLVNAIVFK	162–182	0.1259
63		AMGITDVFSSSANLSGISSAESLK	300–323	0.1239
64		VTEQESKPVKM	201–211	0.1172
65		GITDVFSSSANLSGISSAESLK	302–323	0.1089
66		VASMASEK	200–227	0.1086
67		TSSNVMEER	269–277	0.1050
68		DILNQITKPNDVY	86–98	0.0951
69		LTEWTSSNVMEER	265–277	0.0807
70		ELINSWVESQTN	144–155	0.0798
71		TEWTSSNVMEER	266–277	0.0763
72		LYAEER	106–111	0.0759
73		EAGVDAASVS	347–356	0.0755
74		VASMASEE	220–227	0.0721
75		VTEQESKPVQM	201–211	0.0712
76		TQINK	52–56	0.0607
77		NKVVR	55–59	0.0591
78		VTEQESKPVQMMYQIGLFRVASMASEK	201–227	0.0512
79		NVLKPSSVDSQTAMVLVNAIVFK	160–182	0.0486
80		NVLQPSSVDSQTAMVLVNAIVFK	160–182	0.0365
81		SDFHLFGPPGK *	299–309	0.8619
82		SGYSGAFHCLK *	208–218	0.8239
83		SGAFHCLK *	211–218	0.8038
84		CQLCQGSGGIPPEK *	518–531	0.6874
85		YFGYTGALRCLV *	540–551	0.6541
86		DLLFKDSAIMLK *	216–327	0.6400
87		SGALHCLK *	211–218	0.5971
88		FMMFESQNKDLLFK *	644–657	0.5892
89		YFGYTGALR *	540–548	0.5801
90		KDSNVNWNNLK	458–468	0.4863
91		DDNKVEDIWSFLSK	275–288	0.4641
92		SGGIPPEK	524–531	0.4622
93		NIPIGTLLHRG	145–155	0.4328
94		DLLFKDSAIMLE	316–327	0.4322
95		SAIQSMR	345–351	0.4293
96		ANVMDYR	595–601	0.4255
97		FFSASCVPGATIEQK	174–188	0.4152
98		NIPIGTLLHR	145–154	0.3756
99		TSCHTGLGR	132–140	0.3624
100		GAIEWEGIESGSVEQAVAKFFSASCVPGA	155–183	0.3503
101		FMMFESKNK	644–652	0.3416
102		KDQLTPSPR	352–360	0.3329
103		FMMFESQNK	644–652	0.3265
104		GDVAFVK	222–228	0.3236
105		EAGLAPYK	85–92	0.3173
106		GLIHNR	488–493	0.3124
107	Ovotransferrin (63%)	VEDIWSFLSE	278–288	0.3066
108		GAIEWEGIESGSVEKAVAK	155–173	0.2986
109		DGKGDVAFVK	219–228	0.2939
110		SDFGVDTK	291–298	0.2580
111		AQSDFGVDTK	289–298	0.2525
112		GDVAFIKHSTVEENTGGK	554–571	0.2429
113		TDERPASYF	443–451	0.2356
114		GAIEWEGIESGSVEQAVAK	155–173	0.2308
115		AAHAVVAR	267–274	0.2295
116		GANEWEGIESGSVEQAVAK	155–173	0.2076
117		GAIEWEGNESGSVEQAVAK	155–173	0.2067
118		AQSDFGVDTE	289–298	0.1852
119		FYTVISSLKTCNPS	680–693	0.1792
120		VAAHAVVAR	266–274	0.1704

Table A1. *Cont.*

No.	Egg Protein Sequence Coverage	Peptide	Peptide Sequence Number	Score
		(b) Diphenolase inhibitory activity		
121		GAIEWEGIESGSVEQAVAE	155–173	0.1683
122		FGVHGSEK	634–641	0.1601
123		FGVNGSEKSK	634–643	0.1364
124		RFGVNGSEK	633–641	0.1351
125		GDVAFVQHSTVEENTGGK	554–571	0.1323
126		KGTEFTVNDLQGK	119–131	0.1190
127		GTEFTVNDLQGK	120–131	0.1166
128		DVAFIQHSTVEENTGGK	555–571	0.1158
129		KCVAS	531–535	0.1136
130		TDERPASY	443–450	0.0891
131		LKPIAAEVYEHTEGSTTSYY	93–112	0.0753
132		YTVISSLK	681–688	0.0742
133		CTVVDETK	390–397	0.0495
134		HTTVNENAPDQK	229–240	0.0390
135		FPNATDKEGK	32–41	0.3269
136		VMVLCNR	107–113	0.2887
137		GASVDKR	140–146	0.2203
138		SIEFGTNISK	71–80	0.1899
139		AVVESNGTLTLSHFGK	194–209	0.1597
140	Ovomucoid (38%)	FCNAVVES	191–198	0.1383
141		VEQGASVDKR	137–146	0.0903
142		CAHKVEQ	133–139	0.0902
143		VEQGASVDER	137–146	0.0734
144		CNFCNAVVESNGTLTLSHFGK	189–209	0.0623
145		VEQGASVDK	137–145	0.0585
146		VEQGASVDE	137–145	0.0467
147		SGGQFSLTSTVKVC *	1973–1986	0.5560
148		SSCEDCVCT *	1888–1896	0.5459
149		FNCSSAGPGAIGSEC *	771–785	0.5429
150		SSCICS *	270–275	0.5397
151		FDGRSR *	1000–1005	0.5330
152		PAQEQLM	1255–1261	0.3931
153		KSLSICSLK	916–924	0.3501
154		VTSDGCCK	2001–2008	0.3200
155		LEGCYPECS	1163–1171	0.3088
156	Ovomucin (26%)	ECGNSC	312–317	0.2923
157		EPSELCK	1629–1635	0.2680
158		TCTCNKR	846–852	0.2315
159		DTCADPE	319–325	0.2167
160		VTDSF	1591–1595	0.2004
161		TATGAVEDSAAAFGNSWE	547–564	0.1661
162		GTCSTYS	2044–2050	0.1278
163		IQEIATDPGAEK	941–952	0.1215
164		EVIVDTLLSR	1722–1731	0.1101
165		VQVSTVGR	28–35	0.0990
166		AVTGTN	1901–1906	0.0685
167		GYSLGNWVCAAK *	40–51	0.6563
168		HGLDNYRG	33–40	0.4763
169		HGLDNYR	33–39	0.3753
170		GTDVQAWIR	135–143	0.3365
171	Lysozyme (54%)	GILQINSR	72–79	0.2008
172		FESNFNTQATNR	52–63	0.1820
173		SNFNTQATNR	54–63	0.1487
174		ILQINSR	73–79	0.1212
175		NTDGSTDYGILQINSR	64–79	0.0900
176		VHNLFK	80–85	0.3580
177		HSLELEEFR	354–362	0.2286
178		VATLPAEKMK	220–229	0.1937
179	Ovalbumin-related protein Y (28%)	KFYTGGVEEVNFK	124–136	0.1917
180		VLLPDEVSGLER	244–255	0.1871

Table A1. *Cont.*

No.	Egg Protein Sequence Coverage	Peptide	Peptide Sequence Number	Score
		(b) Diphenolase inhibitory activity		
181		FYTGGVEEVNFK	125–136	0.1570
182		ATGSTGAI	342–349	0.1262
183		TESQMK	50–55	0.0899
184	Ovostatin (2%)	EKMAPALRLLV	538–548	0.4863
185		LVDKDNSPISNK	379–390	0.1410
186		HNPTNTIVYFGR	217–228	0.2810
187	Ovalbumin-related protein X (29%)	ILELPFASGDLSMLVLLPDEVSDLER	74–99	0.1682
188		ILELPFASGDLSMLVLLPDEVSHLER	74–99	0.1607
189		ISQAVHGAFMELSEDGIEMAGSTGVIEDIK	168–197	0.0118

* shortlisted peptides (PeptideRanker score > 0.5) for structure-activity relationship analysis.

References

1. Sánchez-Ferrer, Á.; Rodríguez-López, J.N.; García-Cánovas, F.; García-Carmona, F. Tyrosinase: A comprehensive review of its mechanism. *BBA Protein Struct. Mol. Enzymol.* **1995**, *1247*, 1–11. [CrossRef]

2. Michalek, I.M.; Benn, E.K.; dos Santos, F.L.C.; Gordon, S.; Wen, C.; Liu, B. A systematic review of global legal regulations on the permissible level of heavy metals in cosmetics with particular emphasis on skin lightening products. *Environ. Res.* **2019**, *170*, 187–193. [CrossRef] [PubMed]

3. Westerhof, W.; Kooyers, T.J. Hydroquinone and its analogues in dermatology—A potential health risk. *J. Cosmet Dermatol.* **2005**, *4*, 55–59. [CrossRef] [PubMed]

4. Lee, M.C. Tyrosinase Inhibitor Extract. U.S. Patent 7,125,572, 24 October 2006.

5. Ubeid, A.A.; Zhao, L.; Wang, Y.; Hantash, B.M. Short-sequence oligopeptides with inhibitory activity against mushroom and human tyrosinase. *J. Investig. Dermatol.* **2009**, *129*, 2242–2249. [CrossRef]

6. Kubglomsong, S.; Theerakulkait, C.; Reed, R.L.; Yang, L.; Maier, C.S.; Stevens, J.F. Isolation and identification of tyrosinase-inhibitory and copper-chelating peptides from hydrolyzed rice-bran-derived albumin. *J. Agric. Food Chem.* **2018**, *66*, 8346–8354. [CrossRef] [PubMed]

7. Marini, A.; Farwick, M.; Grether-Beck, S.; Brenden, H.; Felsner, I.; Jaenicke, T.; Weber, M.; Schild, J.; Maczkiewitz, U.; Köhler, T.; et al. Modulation of skin pigmentation by the tetrapeptide PKEK: In vitro and in vivo evidence for skin whitening effects. *Exp. Dermatol.* **2012**, *21*, 140–146. [CrossRef] [PubMed]

8. Albericio, F.; Kruger, H.G. Therapeutic peptides. *Future Med. Chem.* **2012**, *4*, 1527–1531. [CrossRef]

9. Ochiai, A.; Tanaka, S.; Tanaka, T.; Taniguchi, M. Rice bran protein as a potent source of antimelanogenic peptides with tyrosinase inhibitory activity. *J. Nat. Prod.* **2016**, *79*, 2545–2551. [CrossRef]

10. Oh, G.W.; Ko, S.C.; Heo, S.Y.; Nguyen, V.T.; Kim, G.; Jang, C.H.; Park, W.S.; Choi, I.-W.; Qian, Z.-J.; Jung, W.K. A novel peptide purified from the fermented microalga *Pavlova lutheri* attenuates oxidative stress and melanogenesis in B16F10 melanoma cells. *Process. Biochem.* **2015**, *50*, 1318–1326. [CrossRef]

11. Eriksson, L.; Johansson, E.; Kettaneh-Wold, N.; Wikström, C.; Wold, S. D-optimal design. In *Design of Experiments: Principles and Applications*; UMETRICS: Stockholm, Sweden, 2000.

12. Alkali, L.M.T.B.M. D-optimal design optimization of *Jatropha curcas* L. seed oil hydrolysis via alkali-catalyzed reactions. *Sains Malays.* **2012**, *41*, 731–738.

13. Bahadi, M.; Yusoff, M.F.; Derawi, J.S.D. Optimization of response surface methodology by d-optimal design for alkaline hydrolysis of crude palm kernel oil. *Sains Malays.* **2020**, *49*, 29–41. [CrossRef]

14. Olsen, J.V.; Ong, S.E.; Mann, M. Trypsin cleaves exclusively C-terminal to arginine and lysine residues. *Mol. Cell. Proteom.* **2004**, *3*, 608–614. [CrossRef] [PubMed]

15. Blow, D.M. The Structure of Chymotrypsin. In *The Enzymes*, 3rd ed.; Boyer, P.D., Ed.; Academic Press: New York, NY, USA, 1971; pp. 185–212.

16. Hsiao, N.W.; Tseng, T.S.; Lee, Y.C.; Chen, W.C.; Lin, H.H.; Chen, Y.R.; Wang, Y.-T.; Hsu, H.-J.; Tsai, K.C. Serendipitous discovery of short peptides from natural products as tyrosinase inhibitors. *J. Chem. Inf. Model.* **2014**, *54*, 3099–3111. [CrossRef] [PubMed]

17. Schurink, M.; van Berkel, W.J.; Wichers, H.J.; Boeriu, C.G. Novel peptides with tyrosinase inhibitory activity. *Peptides* **2007**, *28*, 485–495. [CrossRef]

18. Miguel, M.; Recio, I.; Gomez-Ruiz, J.A.; Ramos, M.; Lopez-Fandino, R. Angiotensin I–converting enzyme inhibitory activity of peptides derived from egg white proteins by enzymatic hydrolysis. *J. Food Protect.* **2004**, *67*, 1914–1920. [CrossRef]

19. Baharuddin, N.A.; Halim NR, A.; Sarbon, N.M. Effect of degree of hydrolysis (DH) on the functional properties and angiotensin I-converting enzyme (ACE) inhibitory activity of eel (*Monopterus* sp.) protein hydrolysate. *Int. Food Res. J.* **2016**, *23*, 1424–1431.

20. Takahashi, M.; Takara, K.; Toyozato, T.; Wada, K. A novel bioactive chalcone of *Morus australis* inhibits tyrosinase activity and melanin biosynthesis in B16 melanoma cells. *J. Oleo Sci.* **2012**, *61*, 585–592. [CrossRef]

21. Siow, H.L.; Gan, C.Y. Extraction of antioxidative and antihypertensive bioactive peptides from Parkia speciosa seeds. *Food Chem.* **2013**, *141*, 3435–3442. [CrossRef]

22. Ma, B.; Zhang, K.; Hendrie, C.; Liang, C.; Li, M.; Doherty-Kirby, A.; Lajoie, G. PEAKS: Powerful software for peptide de novo sequencing by tandem mass spectrometry. *Rapid Commun. Mass Spectrom.* **2003**, *17*, 2337–2342. [CrossRef]

23. Mooney, C.; Haslam, N.J.; Pollastri, G.; Shields, D.C. Towards the improved discovery and design of functional peptides: Common features of diverse classes permit generalized prediction of bioactivity. *PLoS ONE* **2012**, *7*, e45012. [CrossRef]

24. Trabuco, L.G.; Lise, S.; Petsalaki, E.; Russell, R.B. PepSite: Prediction of peptide-binding sites from protein surfaces. *Nucleic Acids Res.* **2012**, *40*, W423–W427. [CrossRef] [PubMed]

25. Abdou, A.M.; Kim, M.; Sato, K. Functional proteins and peptides of hen's egg origin. In *Bioactive Food Peptides in Health and Disease*; Blanca, H.L., Hsieh, C.C., Eds.; InTech: Rijeka, Croatia, 2013; pp. 115–144.

26. Akazawa, T.; Ogawa, M.; Hayakawa, S. Migration of chicken egg-white protein ovalbumin-related protein X and its alteration in heparin-binding affinity during embryogenesis of fertilized egg. *Poult. Sci.* **2019**, *98*, 5100–5108. [CrossRef] [PubMed]

27. Hirose, J.; Doi, Y.; Kitabatake, N.; Narita, H. Ovalbumin-related gene Y protein bears carbohydrate chains of the ovomucoid type. *Biosci. Biotechnol. Biochem.* **2006**, *70*, 144–151. [CrossRef]

28. Abeyrathne, E.D.N.S.; Lee, H.Y.; Jo, C.; Nam, K.C.; Ahn, D.U. Enzymatic hydrolysis of ovalbumin and the functional properties of the hydrolysates. *Poult. Sci.* **2014**, *93*, 2678–2686. [CrossRef] [PubMed]

29. Stevens, L. Egg white proteins. *Comp. Biochem. Phys. B Comp. Biochem.* **1991**, *100*, 1–9. [CrossRef]

30. Custódio, M.F.; Goulart, A.J.; Marques, D.P.; Giordano, R.C.; Giordano, R.D.L.C.; Monti, R. Hydrolysis of cheese whey proteins with trypsin, chymotrypsin and carboxypeptidase A. *Aliment. Nutr. Araraquara* **2009**, *16*, 105–109.

31. Noh, D.O.; Suh, H.J. Preparation of egg white liquid hydrolysate (ELH) and its radical-scavenging activity. *Prev. Nutr. Food Sci.* **2015**, *20*, 183. [CrossRef]

32. De Castro, R.J.S.; Sato, H.H. A response surface approach on optimization of hydrolysis parameters for the production of egg white protein hydrolysates with antioxidant activities. *Biocatal. Agric. Biotechnol.* **2015**, *4*, 55–62. [CrossRef]

33. Chen, C.; Chi, Y.J.; Zhao, M.Y.; Xu, W. Influence of degree of hydrolysis on functional properties, antioxidant and ACE inhibitory activities of egg white protein hydrolysate. *Food Sci. Biotechnol.* **2012**, *21*, 27–34. [CrossRef]

34. Garg, S.; Apostolopoulos, V.; Nurgali, K.; Mishra, V.K. Evaluation of in silico approach for prediction of presence of opioid peptides in wheat. *J. Funct. Foods* **2018**, *41*, 34–40. [CrossRef]

35. Mudgil, P.; Kamal, H.; Yuen, G.C.; Maqsood, S. Characterization and identification of novel antidiabetic and anti-obesity peptides from camel milk protein hydrolysates. *Food Chem.* **2018**, *259*, 46–54. [CrossRef] [PubMed]

36. Salim MA, S.M.; Gan, C.Y. Dual-function peptides derived from egg white ovalbumin: Bioinformatics identification with validation using in vitro assay. *J. Funct. Foods* **2020**, *64*, 103618.

37. Strothkamp, K.G.; Jolley, R.L.; Mason, H.S. Quaternary structure of mushroom tyrosinase. *Biochem. Bioph. Res. Co.* **1976**, *70*, 519–524.

38. Ismaya, W.T.; Rozeboom, H.J.; Weijn, A.; Mes, J.J.; Fusetti, F.; Wichers, H.J.; Dijkstra, B.W. Crystal structure of Agaricus bisporus mushroom tyrosinase: Identity of the tetramer subunits and interaction with tropolone. *Biochemistry* **2011**, *50*, 5477–5486.

39. Drickamer, K.; Taylor, M.E. Recent insights into structures and functions of C-type lectins in the immune system. *Curr. Opin. Struct. Biol.* **2015**, *34*, 26–34. [PubMed]

40. Weijn, A.; Bastiaan-Net, S.; Wichers, H.J.; Mes, J.J. Melanin biosynthesis pathway in *Agaricus bisporus* mushrooms. *Fungal Genet. Biol.* **2013**, *55*, 42–53.

41. Flurkey, W.H.; Inlow, J.K. Proteolytic processing of polyphenol oxidase from plants and fungi. *J. Inorg. Biochem.* **2008**, *102*, 2160–2170. [CrossRef]

42. Kanteev, M.; Goldfeder, M.; Fishman, A. Structure–function correlations in tyrosinases. *Protein Sci.* **2015**, *24*, 1360–1369.

43. Valley, C.C.; Cembran, A.; Perlmutter, J.D.; Lewis, A.K.; Labello, N.P.; Gao, J.; Sachs, J.N. The methionine-aromatic motif plays a unique role in stabilizing protein structure. *J. Biol. Chem.* **2012**, *287*, 34979–34991.

44. Kanteev, M.; Goldfeder, M.; Chojnacki, M.; Adir, N.; Fishman, A. The mechanism of copper uptake by tyrosinase from *Bacillus megaterium*. *JBIC J. Biol. Inorg. Chem.* **2013**, *18*, 895–903.

45. Hassani, S.; Haghbeen, K.; Fazli, M. Non-specific binding sites help to explain mixed inhibition in mushroom tyrosinase activities. *Eur. J. Med. Chem.* **2016**, *122*, 138–148. [CrossRef] [PubMed]

46. Jung, H.J.; Noh, S.G.; Park, Y.; Kang, D.; Chun, P.; Chung, H.Y.; Moon, H.R. In vitro and in silico insights into tyrosinase inhibitors with (E)-benzylidene-1-indanone derivatives. *Comput. Struct. Biotechnol. J.* **2019**, *17*, 1255–1264. [CrossRef] [PubMed]